3. Intact Rock Strength

Introduction

A starting point for a discussion on the mechanical properties of rock and rock masses is the following statement by Palmström (1995): “A rock mass is a material quite different from other structural materials used in civil engineering. It is heterogeneous and quite often discontinuous, but it is one of the materials in the earth's crust, which is most used in man's construction.”

Geologists describe, classify and name rocks based on their mode of origin, colour, texture, fabric, and history rather than based on their strength or other mechanical characteristics. Often multiple rock units are then grouped together into formations based on lithology or age relationships. Classically, formation boundaries in bedded sedimentary units are stratigraphically delineated by specific depositional time horizons. Such divisions are often more complex in igneous and metamorphic terrains. Geologists commonly also subdivide rock names based on an abundance of a particular type of mineral within the rock or based on fabric pervasiveness, degree of metamorphism or alteration.

It is typical for geologists to define three main types of rocks – igneous, sedimentary, and metamorphic, based on their general mode of origin – igneous rocks being derived directly from the cooling of molten magma; sedimentary rocks being generally derived from deposited accumulations of reworked older debris and metamorphic rocks created through significant pressure and temperature change to other rocks. A summary of these different rock types is given in Table 1 in Appendix 1, which also includes a more detailed discussion on the definitions.

Practical and reliable methods for collecting, preparing, and testing samples of intact rock subjected to triaxial compressive and tensile loading to failure are described in Appendix 2 to this chapter. The aim in this appendix is to describe methods and equipment that can be used in both the laboratory and in the field to generate reliable information that can be incorporated into the interpretation of rock and rock mass behaviour models. Wherever possible, the simplest equipment that can be used to provide reliable basic information has been chosen to present a practical introduction to students and graduates entering the field of rock engineering for the first time and to geologists, engineering geologists and engineers already working in the field. Undoubtedly, those involved in research into more detailed aspects of rock and rock mass behaviour may need to use more sophisticated equipment and techniques, which are not discussed in this chapter.

The mechanical behaviour of intact rock samples when subjected to stress is the principal topic of discussion in this chapter. High quality testing of intact rock samples has been going on for at least the past seventy years. This has been prompted by the need to understand rock deformation and failure processes related to applications involving the use of rock as an engineering material in tunnels, mining excavations, slopes, and foundations. It is strongly recommended that laboratory testing of intact rock, as described in this chapter, should be a required component of any project involving the design and construction of significant tunnels, shafts, caverns, slopes, or foundations in rock.

The basic mechanics of rock failure are discussed, with particular attention to the determination of the tensile strength of intact rock. Two tables dealing with textural and origin-based classification and with average values of intact rock modulus, uniaxial compressive strength and the Hoek-Brown m_i constant have been included in the text. These tables are to assist readers who may need to understand some of the issues discussed and who may have difficulty in finding reliable classifications and engineering properties of typical rocks in available literature.

Triaxial confining stresses for intact rock testing

In the context of this discussion, the stresses to which intact rock can be subjected are those associated with the construction of slopes, tunnels, caverns and foundations in rock and rock masses. Failure of the intact rock is one of the critical components which define the failure on rock masses in any of these structures. The highest excavated slopes are typically those in large open pit mines in which pit depths are currently limited to about 1000 m which means that the vertical gravitational stress is approximately 27 MPa at the base of the pit. Deep level underground mines are currently approaching 4000 m in depth, and this means that vertical gravitational stresses of about 100 MPa need to be considered in relation to intact rock strength.

The intact uniaxial compressive strength of rock ranges from about 25 to 50 MPa for sedimentary rock such as claystone, chalk and siltstone and 200 to 400 MPa for igneous rocks such as basalt, diabase and dolerite. These strengths may increase by factors of 3 to 5 with confinement. Hence, in designing triaxial test equipment for a rock mechanics laboratory to cover the full range of stresses which maybe encountered in mining, axial stresses of up to 1000 MPa and confining pressures of up to 50 MPa are required. For 50 mm diameter core samples, this means that a testing machine or loading frame with a capacity of 250 tons should be considered for a rock mechanics laboratory.

The confining stresses used to establish the strength of intact rock should consider the confining stresses anticipated in the problem being analyzed. For example, in the 1000 m high pit slope wall, slope failures are relatively shallow and confining stresses in the failed region are much less than the vertical stress at the bottom of the pit. In an underground mine, confining stresses are increased by the extraction of ore. Because the failure of intact rock discussed in this chapter is analyzed using an empirical criterion, the Hoek-Brown parameters should be determined at confining stresses that are appropriate for the problem being analyzed.

Selection of samples for determining Hoek-Brown criterion for intact rock

Note that this chapter deals with establishing the strength for isotropic homogeneous intact rock specimens only. Laboratory strength results for intact specimens may be significantly affected by the presence of defects such as veins, fractures and inclusions. Such strength results for defected samples when grouped with results from intact rock samples can produce a wide scatter in strength results often resulting in bi-modal strength distributions. Bewick et al (2015) and Bewick et al (2019) provides guidance on grouping the failure mode observed in samples containing defects and separating those groups for analysis. It is essential that results from defected samples are not included when establishing the

Hoek-Brown criterion for isotropic homogeneous intact rock. Figure 1 illustrates the selection of isotropic intact samples from a diamond drill core, chosen to eliminate the impact of defects.

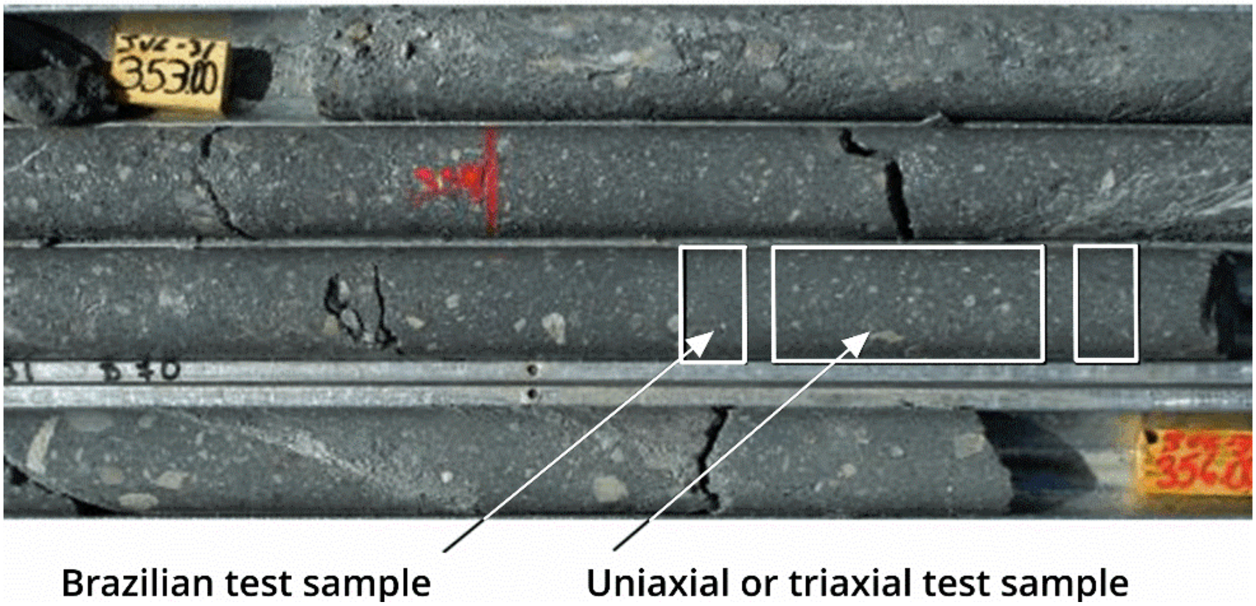

Figure 1: Selection of isotropic intact samples of diamond drill core for testing.

The Hoek-Brown failure criterion

Hoek and Brown (1980) describe the development of the Hoek-Brown failure criterion as a trial-and-error process using Griffith (1924) theory as a starting point. They were seeking an empirical relationship that fitted observed failure conditions for brittle rock subjected to compressive stresses, such as the shear failures illustrated in Figure 2. The equation chosen to represent the failure of intact rock was:

$$\sigma_1 = \sigma_3 + \sigma_c \sqrt{m_i \frac{\sigma_3}{\sigma_c} + 1} \tag{1}$$

where σ_c is the uniaxial compressive strength of the material and m_i is a material constant which defines the brittleness of intact rock.

The general solution for a Mohr envelope was published by Balmer (1952). Hoek et al (2002) published a solution which expresses the normal and shear stresses in terms of the corresponding principal stresses as follows:

$$\sigma = \frac{(\sigma_1+\sigma_3)}{2} - \frac{(\sigma_1-\sigma_3)}{2} \cdot \frac{\partial\sigma_1/\partial\sigma_3 - 1}{\partial\sigma_1/\partial\sigma_3 + 1} \qquad (2)$$

$$\tau = (\sigma_1 - \sigma_3)\frac{\sqrt{\partial\sigma_1/\partial\sigma_3}}{\partial\sigma_1/\partial\sigma_3 + 1} \qquad (3)$$

$$\frac{\partial\sigma_1}{\partial\sigma_3} = 1 + \frac{m_i\sigma_c}{2\sqrt{m_i\sigma_3/\sigma_c + 1}} \qquad (4)$$

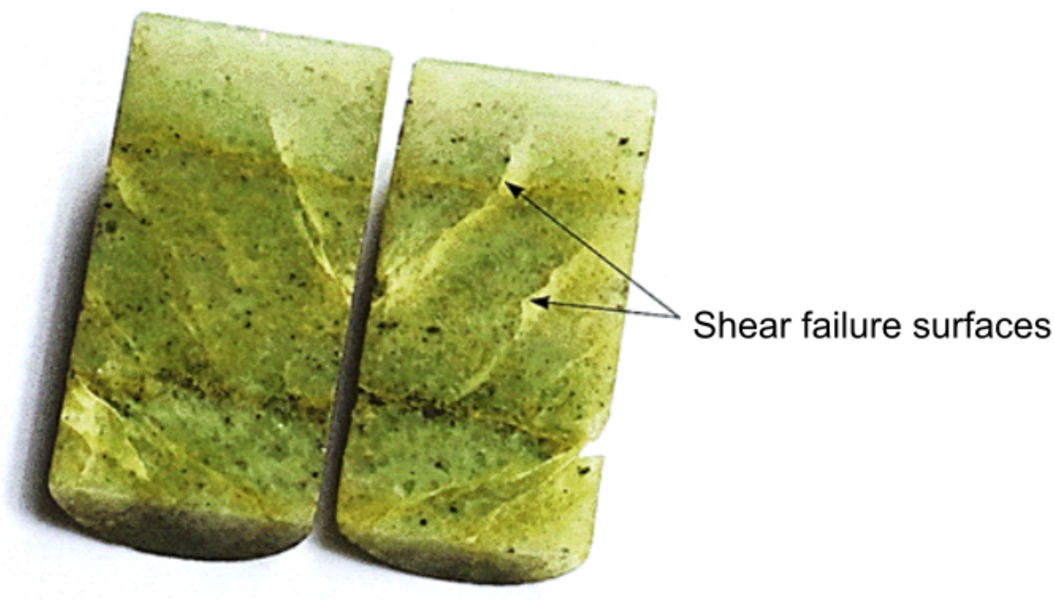

Figure 2: Fine grained granite triaxial test specimen with shear failure surfaces. This specimen was cut into two pieces after removal from a triaxial cell. It had been loaded to approximtely 80% of the failure stresses, so that the shear failures had developed, but the specimen had not failed. Tested by Evert Hoek in 1965.

Figure 3 presents an example of a triaxial test program carried out by Schwartz in 1964 as part of a research effort in the USA to investigate the mechanisms of earthquake generation. High quality testing was carried out at several universities and research institutes and a summary of this work can be found in Judd (1964). It is clear, from Figure 3, that the triaxial test data reported by Schwartz is the result of high-quality testing and the careful selection of the acceptable data points. Only a single point is presented for each confining pressure, including the uniaxial compressive strength, resulting in very simple fitting of the Hoek Brown criterion.

It is also clear, from the data presented by Schwartz, that there is a sharp distinction between the shear failure process, to which the Hoek-Brown criterion applies, and the ductile failure process, which is adequately described by the linear Mohr-Coulomb criterion. The brittle-ductile transition for this data set is defined by $\sigma_1/\sigma_3 = 4.5$, as shown in Figure 3.

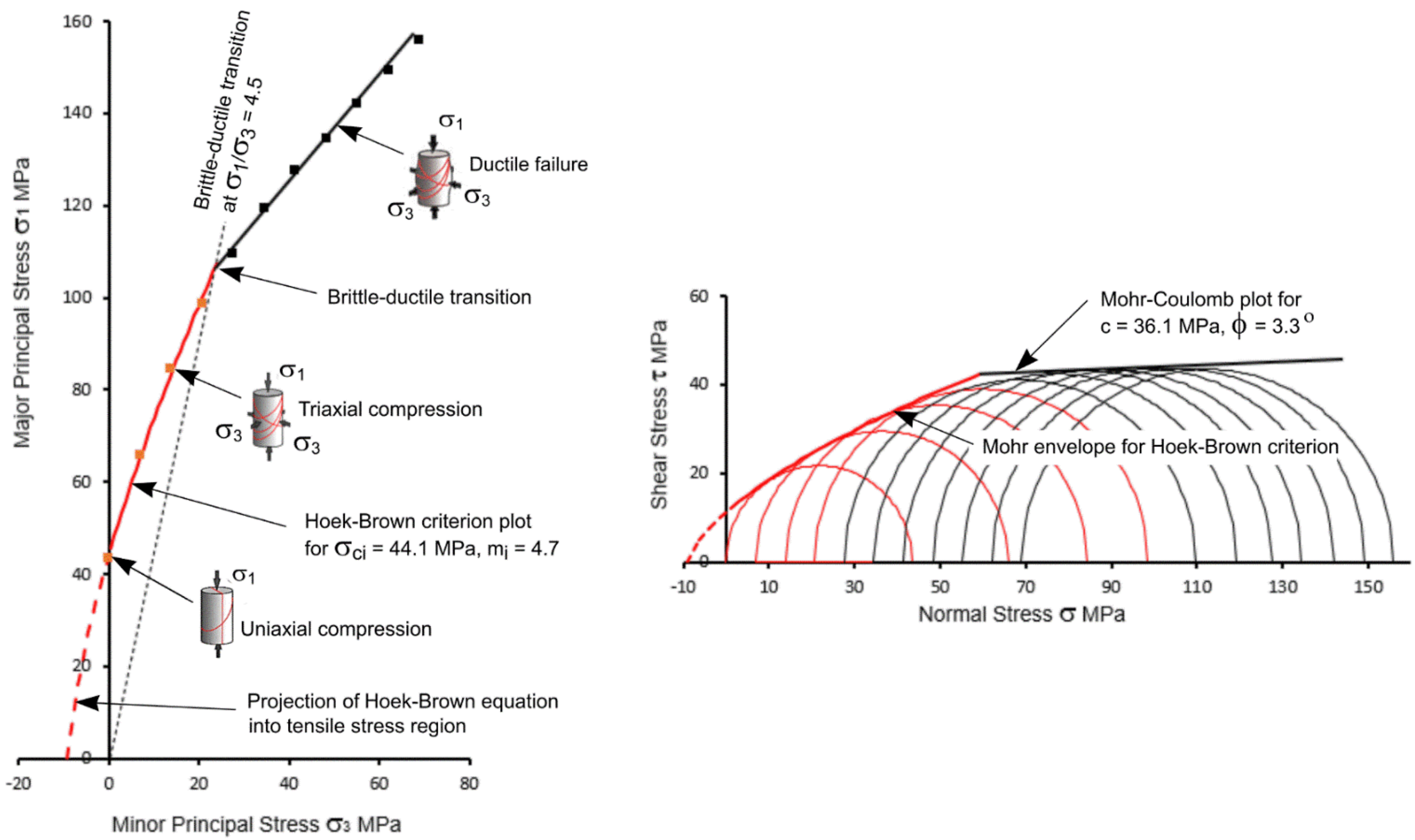

Figure 3: Analysis of triaxial test results on Indiana Limestone by Schwartz (1964). The Hoek-Brown criterion is only applicable to the range, plotted as a red line, between the uniaxial compressive stress ($\sigma_3 = 0$, $\sigma_1 = 43.45$) and the brittle-ductile transition at $\sigma_1/\sigma_3 = 4.5$

One of the main problems with compressive strength testing is the unreliability of the uniaxial test which is carried out with zero applied confining pressure. This occurs at the transition between compressive shear failure and tensile splitting failure of the intact rock. Chakraborty et al (2019) describe the various failure modes that are observed in uniaxial testing, which are illustrated in Figure 4. The Hoek-Brown criterion is only applicable to shear failure, and it is important, when interpreting the results of triaxial tests, to attempt to remove the results of tests exhibiting other types of failure from the data base.

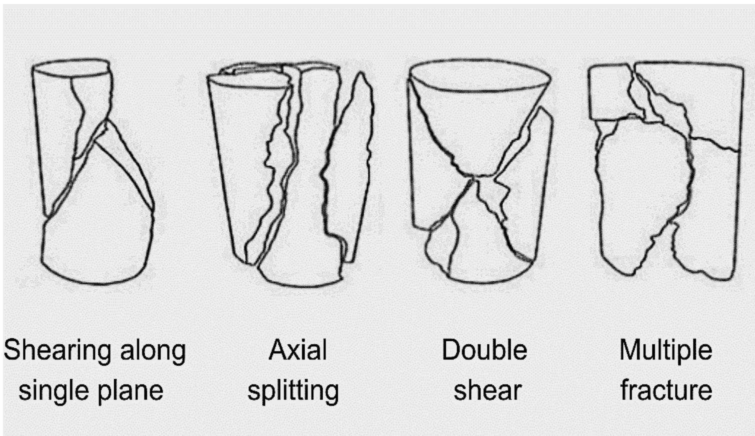

Figure 4: Shear failure, axial splitting and more complex failure modes observed in uniaxial compression testing. Adapted from Chakraborty et al (2019).

Mogi (1966), Byerlee (1968), Scholtz (1968), Evans et al (2013), Hu et al (2018) and many others have all researched the transition from brittle to ductile failure in intact rock and have written about this topic. In general, the transition occurs in the range $3 < \sigma_1/\sigma_3 < 5$ and this range is adequately accurate for most rock engineering design purposes. Where greater precision is required, it is prudent to carry out a test program of the type illustrated in Figure 3.

During the early years in the development of the current triaxial testing methodology, most of the tests were performed by, or under, the supervision of the developers of the equipment as described by Schwartz (1964), Brace (1964), Murrell (1965), and Hoek and Franklin (1968). This meant that the results of non-acceptable failure modes could be deleted based on direct examination of the specimens. In subsequent years, most testing was carried out in commercial laboratories, and it became more difficult to determine and remove those tests which did not exhibit pure shear failure along a single plane. Consequently, it is necessary to establish a methodology to minimize errors resulting from the inclusion of inappropriate data.

A triaxial testing program for intact rock should include a minimum of 3, but preferably 5 triaxial tests, in addition to the uniaxial compressive tests. Ideally, several tests should be carried out at each confining pressure or minor principal stress σ_3 value, as shown in Figure 4. Typically, a greater number of uniaxial test results will be available than the triaxial results and, to carry out a meaningful statistical analysis, a normal distribution curve for each confining pressure should be constructed. The mean and standard deviations of these distribution can then be used as input in the curve fitting process required to determine the uniaxial compressive strength and the value of the Hoek-Brown constant m_i

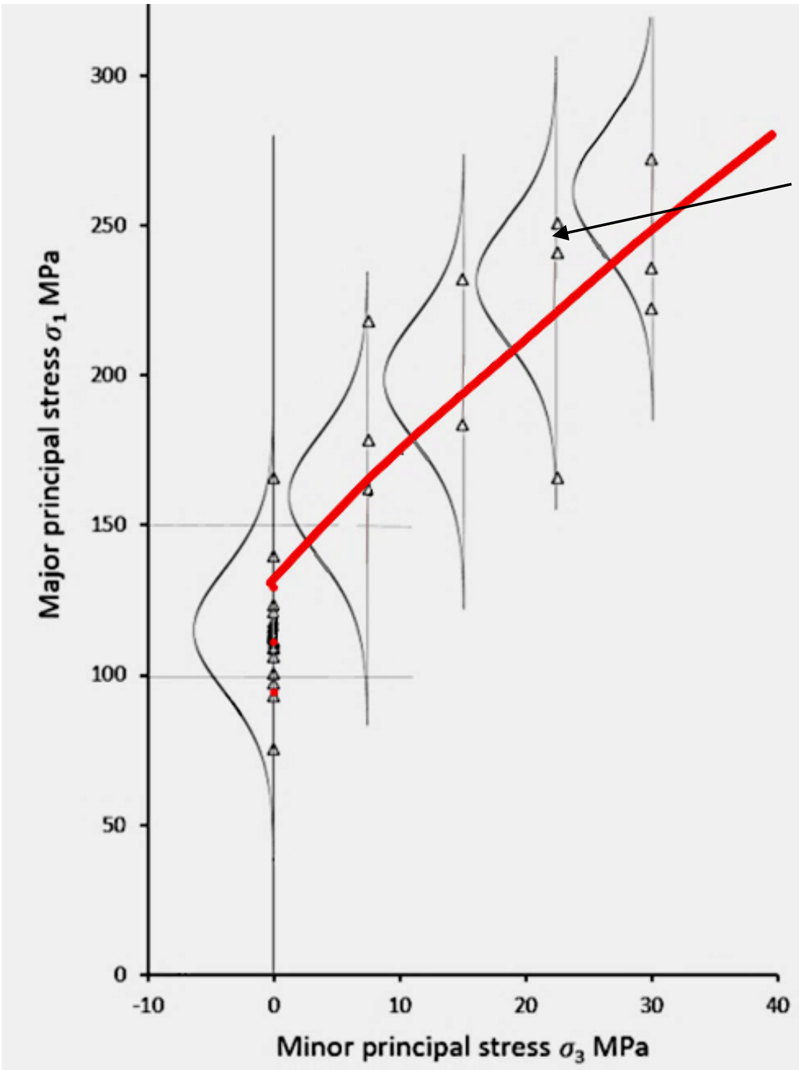

Regression analysis with major principal stresses for each confining pressure defined by a normal distribution. The mean values and standard deviations for each confining pressure are listed below and a regression analysis, gives Hoek-Brown values of σ_{ci} = 130.4 MPa and m_i = 8.1.

σ_3	σ_1
0	115.3
0	116.3
0	117.8
7.5	162.3
7.5	178.5
7.5	218
15	183.6
15	196.8
15	232.1
22.5	165.8
22.5	240.7
22.5	250.9
30	222.3
30	235.7
30	272.4

Figure 5: Analysis of uniaxial and triaxial tests on Coburg Limestone.

Tensile strength of intact rock

Perras and Diederichs (2014) wrote: "Despite the importance of tensile capacity in controlling many failure processes, tensile strength determination is often overlooked in engineering practice due to difficulties with obtaining reliable results." They went on to say: "To date direct tensile testing is regarded as the most valid method for determining the true tensile strength of rock since there are minimal outside influences when the test is completed properly, (Hoek 1964)." Brace (1964) described the best shape for direct tensile specimens to be the "dog bone shape."

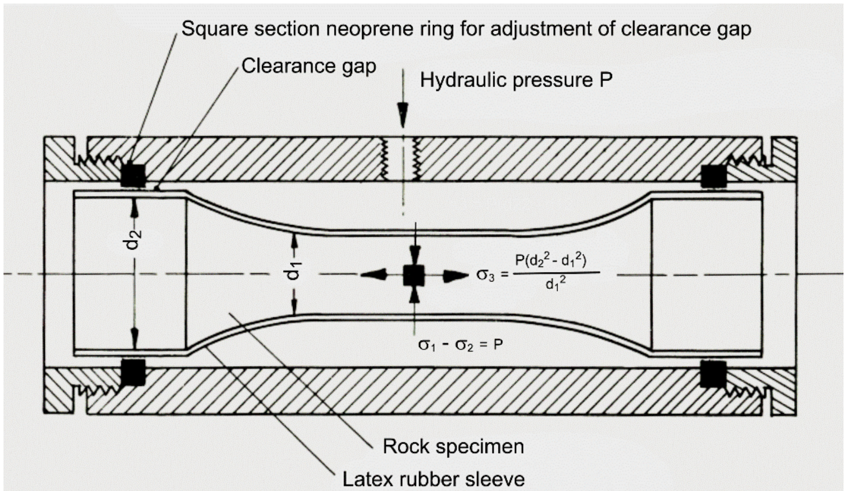

Figure 6: Dogbone specimen used for the determination of the tensile strength of intact rock from Hoek (1965).

Hoek (1965) used the apparatus illustrated in Figure 6 to determine the tensile strength of intact rock. The design of this equipment was based on that used by Brace (1964) in all his triaxial tests on intact rock. The uniformity of the stresses induced in the central section of the dogbone specimen is illustrated in Figure 7 which shows the results of an axisymmetric finite element analysis of the stresses induced by the application of a confining pressure of 10 MPa.

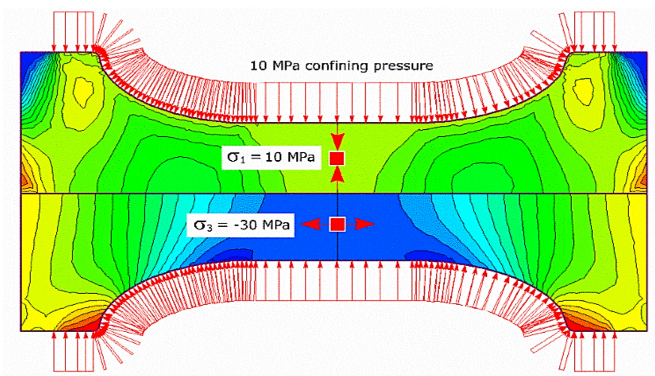

Figure 7: Analysis of stresses induced in the test section of a dog-bone shaped specimen subjected to lateral confining pressure with no axial load applied. The ends of the specimen illustrated are twice the diameter of the central test section.

Ramsey and Chester (2004) and Bobich (2005) investigated the tensile behaviour of Carrara marble in a series of experiments in which they used dogbone shaped specimens like that shown in Figure 7. The results obtained by Ramsey and Chester are well defined by Fairhurst's generalization of Griffith's theory of brittle failure (Fairhurst, 1964). A detailed plot of Ramsey and Chester's test results is given in Figure 9, together with the values of the stresses measured in their experiments.

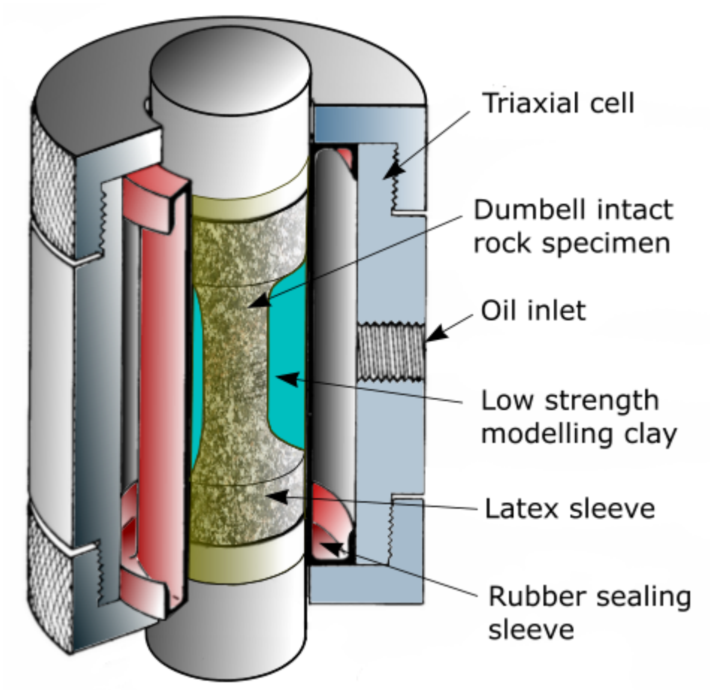

Figure 8: Equipment for confined tensile testing of dog-bone shaped intact rock specimens (based on method used by Ramsey and Chester, 2004). Deformation of the modelling clay, surrounding the reduced section of the specimen, applies a uniform confining pressure. The pressure acting on the enlarged ends induces a tensile stress in the reduced section as shown in Figure 7.

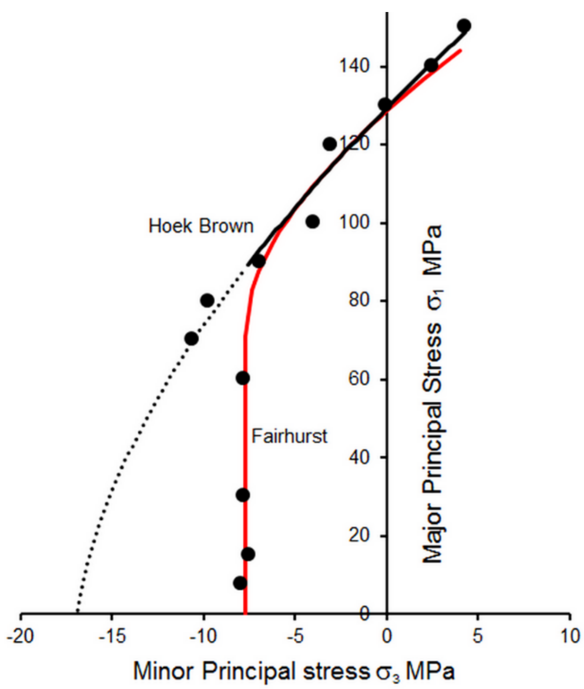

σ_3 MPa	σ_1 MPa	
-7.9	7.5	
-7.5	15.0	TENSILE FAILURE
-7.8	30.0	
-7.8	60.0	
-10.6	70.0	
-9.8	80.0	
-6.9	90.0	TRANSITION FAILURE
-4.0	100.0	
-3.0	120.0	
0.0	130.0	
2.5	140.0	SHEAR FAILURE
4.3	150.0	

Figure 9: Results of confined tensile tests on Carrara Marble by Ramsey and Chester (2004) showing both the Hoek-Brown and Generalized Fairhurst Griffith Theory (in red) fitted plots.

Fairhurst's generalisation of Griffith's $\sigma_{ci}/|\sigma_t|$, where σ_{ci} is the unconfined compressive strength determined by regression analysis

Defining $w = \sqrt{\frac{\sigma_{ci}}{|\sigma_t|} + 1}$, $A = 2(w-1)^2$, $B = \left(\frac{w-1}{2}\right)^2 - 1$

If $\sigma_1/\sigma_3 \leq -w(w-2)$, tensile failure occurs when $\sigma_3 \leq \sigma_t$
If $\sigma_1/\sigma_3 \geq -w(w-2)$, transition between tensile and shear failure occurs when

$$\sigma_1 = \frac{1}{2}\left((2\sigma_3 - A\sigma_t) + \sqrt{(A\sigma_t - 2\sigma_3)^2 - 4(\sigma_3^2 + A\sigma_t\sigma_3 + 2AB\sigma_t^2)}\right) \tag{5}$$

The equivalent relationship for shear and normal stresses is

$$\tau^2 = |\sigma_t|(|\sigma_t| + \sigma_n)(w-1)^2 \tag{6}$$

As shown in Figure 9, only two low confinement triaxial compressive test values are included in the results obtained by Ramsey and Chester. These do not permit an extrapolation of the Hoek-Brown failure curve to higher confinement values as shown in Figure 10. However, by normalizing the results of Ramsey and Chester's tests, as well as triaxial test results on Carrara marble by Franklin and Hoek (1970), it is possible to arrive at the approximate composite curve in Figure 9.

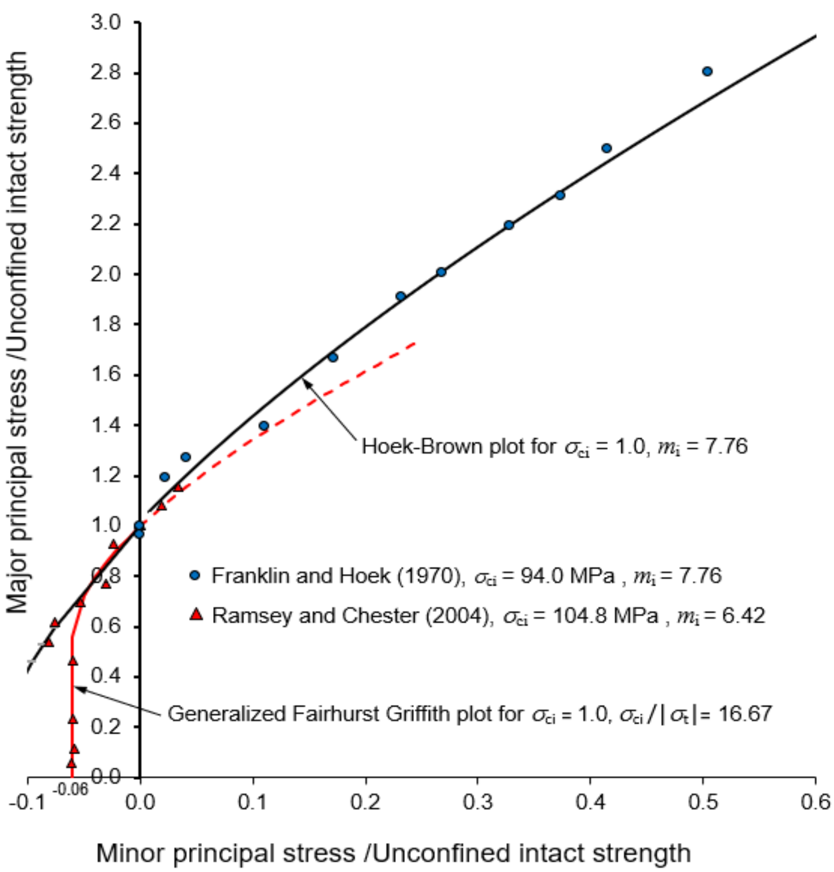

Figure 10: Transition from the Generalized Fairhurst Griffith theory to the Hoek-Brown failure criterion.

To generalize the plot shown in Figure 10, an Excel spreadsheet was prepared[1] in which a Griffith plot, tangential to the Hoek Brown plot for a chosen value of mi, was created. A series of tensile strengths defined by several Griffith plots were then used to plot the mi versus $\sigma_{ci}/|\sigma_t|$ curve presented in Figure 11. Reliable published values of the $\sigma_{ci}/|\sigma_t|$ ratios for a variety of rocks, included in the same plot, confirm the validity of the equation included in Figure 11.

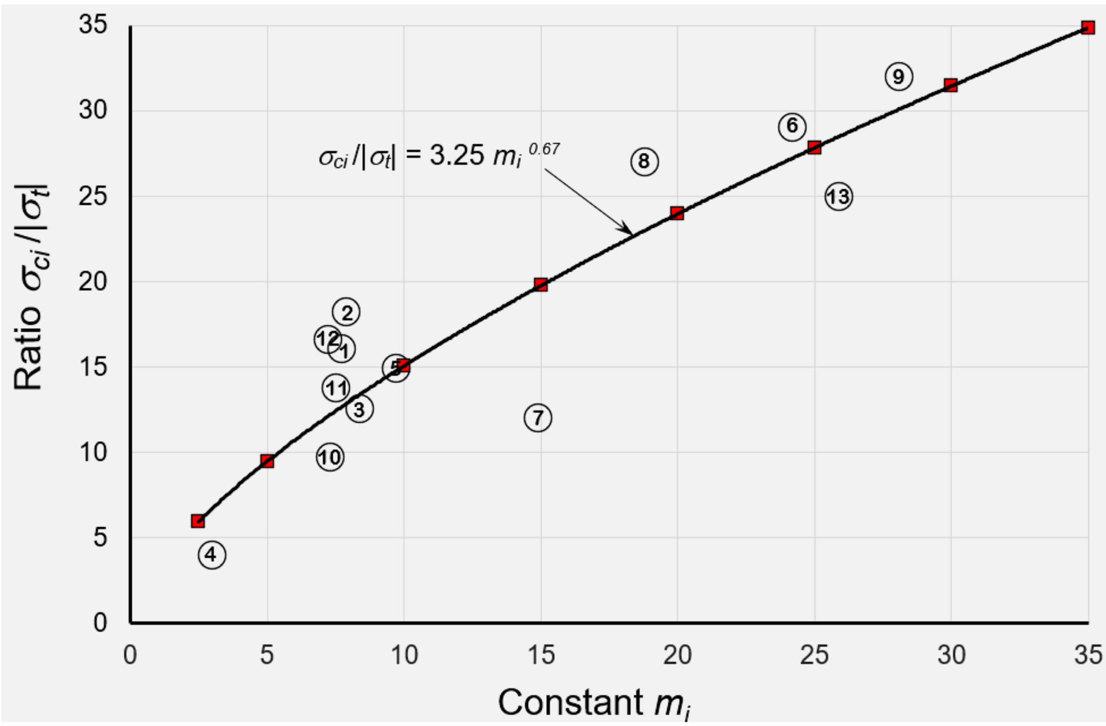

Point	Rock	σci MPa	σt MPa	m_i	σci/|σt|	Reference
1	Gosford Sandstone	72.4	-4.5	7.7	16.1	Brace (1964)
2	Webtuck Dolomite	121.4	-6.64	7.9	18.2	Brace (1964)
3	Blair Dolomite	473.9	-37	8.37	12.54	Brace (1964)
4	Longmaxi Shale	22	-5.5	3	4	Lan et al (2019)
5	Berea Sandstone	102	-6.4	9.7	14.9	Bobich (2005)
7	Witwatersrand Quartzite	226.6	-18.6	14.9	12	Hoek (1965)
6	Bowral Trachyte	200	-7.6	24.2	29	Brace (1964)
8	South African Aplite	600.4	-22.2	18.8	27	Hoek (1965)
9	Lac du Bonnet Granite	224	-7	28.1	32	Martin (1997)
10	Westerly Granite	225	-23.2	7.28	9.7	Brace (1963)
11	Marble	111	-8.07	7.5	13.8	Ros and Eichinger (1928)
12	Carrara Marble	104	-7.7	7.2	16.6	Hoek and Martin (2014)
13	Pottsville sandstone	75.1	-3	25.9	25	Schwartz (1964)

Figure 11: Plot illustrating fitted Hoek-Brown plots for triaxial tests for a range of mi values with the tension cutoff as a function of the mi constant.

[1] This analysis was performed by Dr Connor Langford.

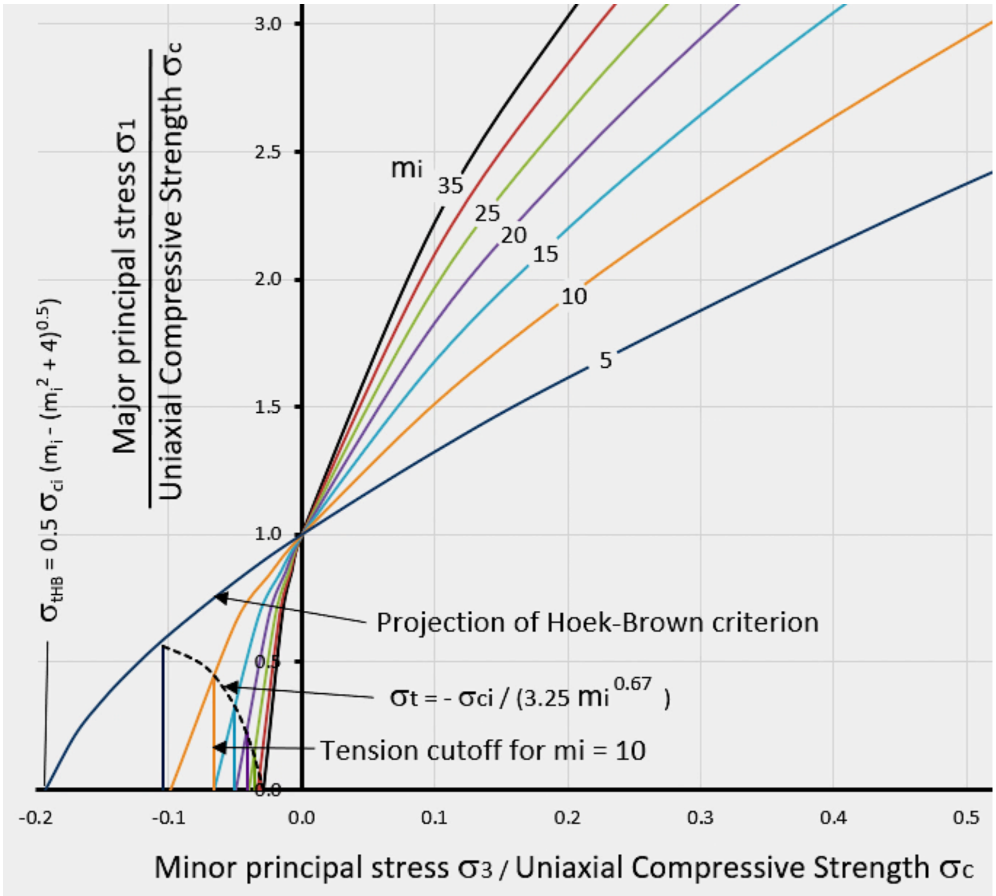

Figure 12: Plot of tension cutoff values for a range of Hoek-Brown curves.

Hoek and Brown (1980) suggested that the tensile strength of intact rock could be estimated from the intercept of the Hoek-Brown curve and the minimum principal stress axis, as shown in Figure 12. This value is defined by the equation:

$$\sigma_{tHB} = 0.5\sigma_{Ci}\left(m_i - \sqrt{m_i^2 + 4}\right) \tag{7}$$

Experimental results, such as those presented in Figures 11 and 12 show that this suggestion was incorrect and that the actual tensile strength σ_t can be calculated more realistically from the empirical, equation numbered, 5, shown below and included in Figures 11 and 12:

$$\sigma_t = -\ \sigma_{ci} / (0.325\ m_i^{\ 0.67}) \tag{8}$$

Equation 8 was derived from a curve fitting analysis of the data on 13 rock types, listed in Figure 11. These results are considered to be the most reliable currently available and it is probable that, as more results of this type become available, the constants in Equation 7 and, perhaps, the form of the equation itself will change. Hence, this equation should be regarded as the best interim solution available rather than a final solution.

Brazilian tests for estimating tensile strength

Relatively few laboratories have access to the full range of equipment required to determine the tensile strength of intact rock dogbone specimens, as described in Figures 6 and 8. Consequently, estimates are frequently made by using a test known as the Brazilian test, in which a disc of intact rock is loaded across its diameter, as shown in Figure 13.

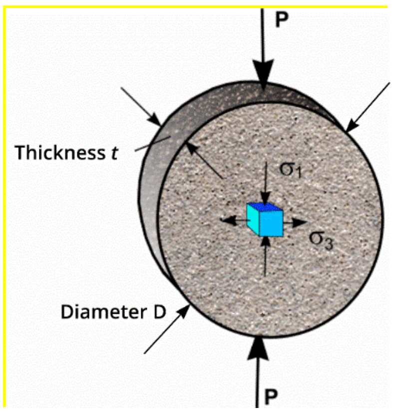

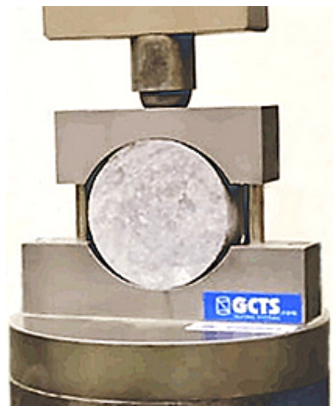

Figure 13: A Brazilian tensile test in which a disc of intact rock, cut from a diamond drilled core, is subjected to a load P across its diameter. As shown on the left, the disc has a diameter D, a thickness *t*, typically one-half the diameter. The Brazilian tensile strength (BTS) is calculated from equation 6, presented below. The photograph on the right illustrates a Brazilian test setup in the University of Alberta, Civil and Environmental Engineering, School of Mining and Petroleum Engineering.

$$St = s3 = -2P/piDT \tag{9}$$

The tensile strength σ_t is estimated from Equation 9 when the applied load P is high enough to induce tensile splitting along the vertical diameter. Perras and Diederichs (2014) show, in Figure 14, that estimates of the ratio of direct tensile tests (DTS) to Brazilian tensile test (BTS) estimates are widely distributed.

Differences between tests on metamorphic, sedimentary, and igneous rocks overlap to the extent that they are not particularly useful in providing clear and reliable guidelines on DTS/BTS values for each of the three categories.

However, Perras and Diederichs suggest that DTS/BTS ratios of 0.86, 0.82 and 0.70 for metamorphic, sedimentary, and igneous rocks provide approximate estimates of the DTS from BTS test results. Figure 13 shows an alternative interpretation, provided by Carter (2021), in which the ratio of DTS/BTS is plotted against the Hoek-Brown constant m_i, giving a similar wide scatter or results but indicating a trend for less variation for rocks with high m_i values.

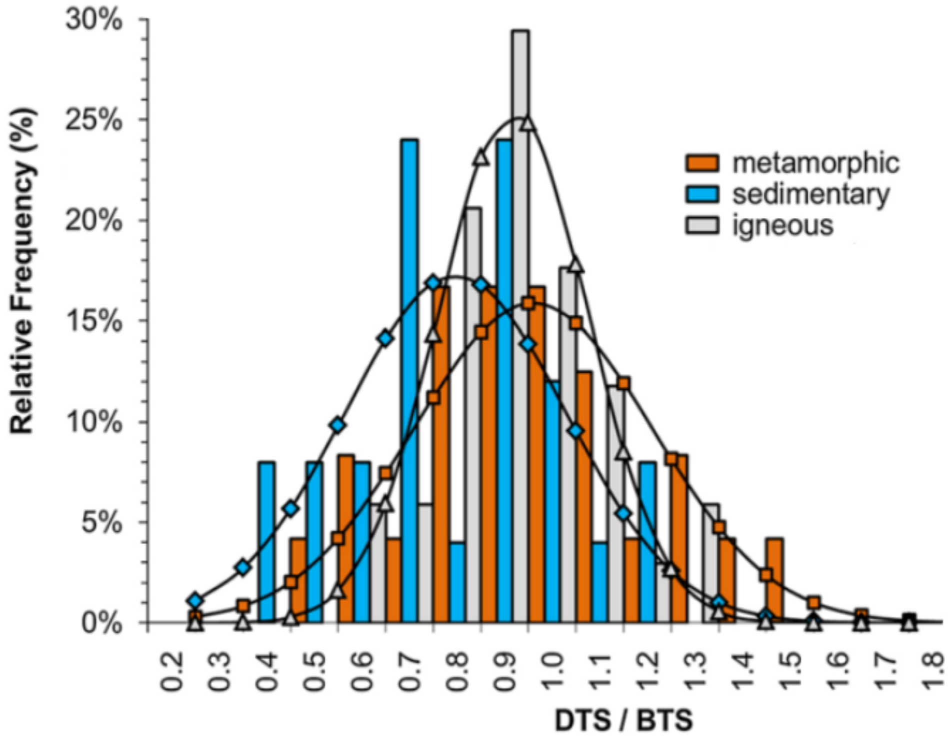

Figure 14: Histogram of the ratio between DTS and BTS for the main rock types.

Brittle shear and tensile failure predicted by the Hoek-Brown criterion

For application in the analysis of practical rock engineering problems, such as tensile failure and spalling in tunnels, it is necessary to simplify the Hoek-Brown failure criterion to the maximum extent possible. Maintaining the accuracy and reliability of the criterion is essential in this simplification process. Figure 14 presents such a simplification in which the Hoek-Brown criterion for brittle shear failure is combined with the criterion for tensile failure, summarized in Equation 5 and Figures 9 and 10.

Throughout this chapter it has been emphasized that the Hoek-Brown criterion is only valid for the brittle shear failure of rock, as shown in Figure 2. However, Figure 10 shows that a backward projection of the curve generated by Equation 1 is very close to the curve generated by the Fairhurst generalized Griffith plot (Equation 2) for the region between the uniaxial compressive strength and the tensile cutoff, defined by Equation 6. Consequently, in developing the simplified plot presented in Figure 14, it has been assumed that an acceptably small error will be generated by the backward projection of the Hoek-Brown curve to link the uniaxial compressive strength to the tensile cutoff, defined by Equation 6.

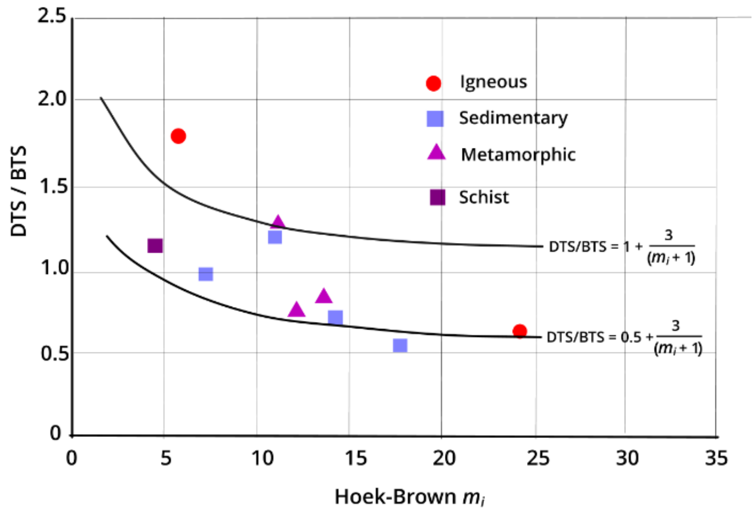

Figure 15: Ratio of DTS/BTS for different m_i values. After Carter (2021).

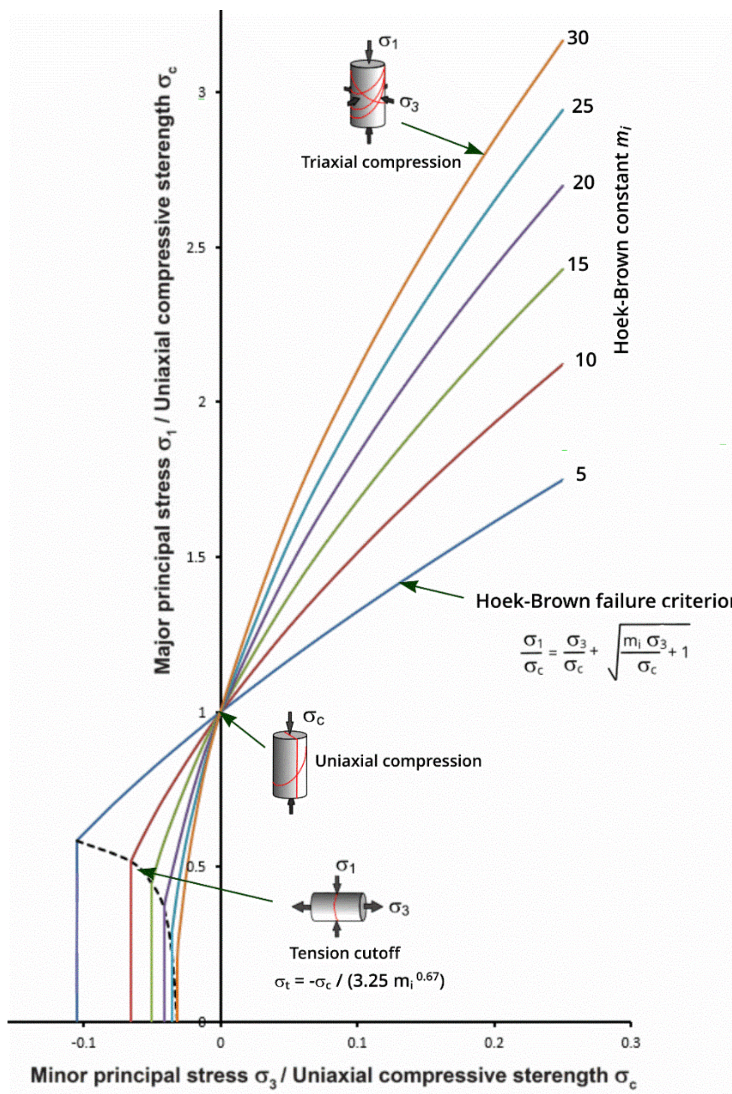

Figure 16: Dimensionless Hoek-Brown criterion plot, with tension cut-off.

Variability of Strength, Stiffness and Hoek-Brown m_i with rock type composition

In the preceding sections variability in intact strength over the range from tensile through shear to ductile failure in compression have been examined. An additional useful measure for characterizing rock types is stiffness, defined in this context by intact Young's Modulus, E_i, the measured tangent to the slope of the stress-strain curve at 50% strain to failure. However, natural rock types are seldom uniform and homogeneous and wide ranges in measured values of these key governing parameters will be determined if a comprehensive laboratory testing program is undertaken. As an example, Figure 17 shows the distribution curves obtained from high quality uniaxial compressive tests on intact samples from the rock mass in which the tunnels and caverns were excavated for the Ingula Pumped Storage Project in South Africa.

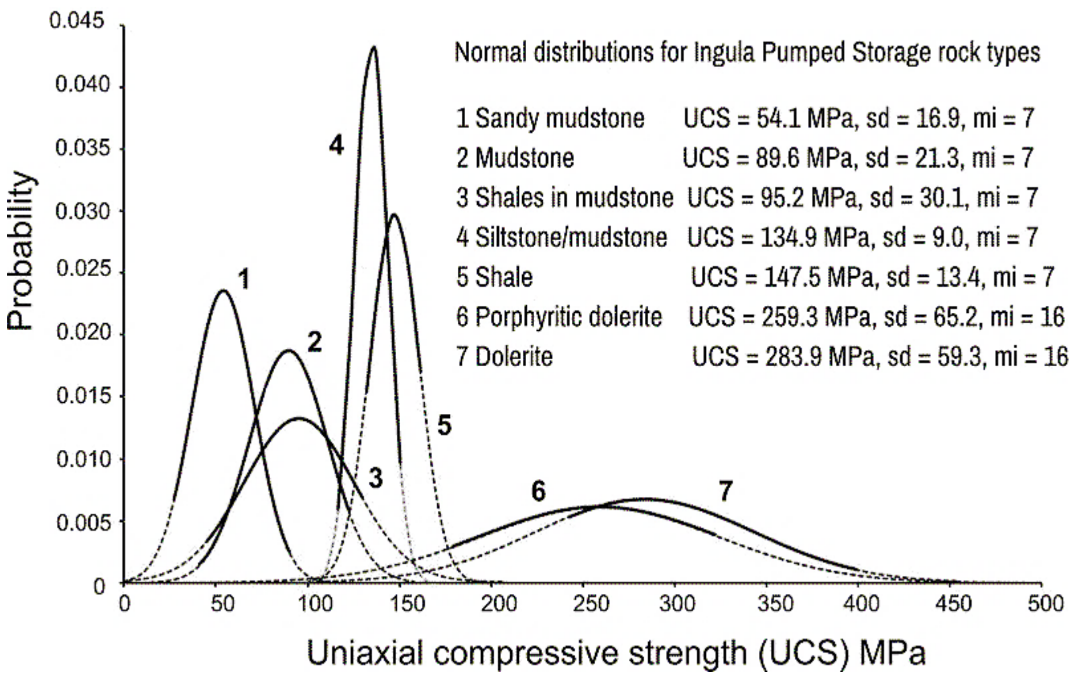

Figure 17: Results of uniaxial compressive strength tests on 7 rock types from the site of the Ingula Pumped Storage Project in South Africa, carried out in the laboratory of the rock mechanics division of the Council for Scientific and Industrial Research. Keyter et al. (2008).

Figure 18 defines each of the 42 rocktypes, derived from Hoek (1999) and Hoek and Diederichs (2006), providing typical ranges the intact modulus E_i, the uniaxial compressive strength σ_{ci} and the Hoek-Brown constant m_i. The rocktypes are subdivided not just by their igneous, sedimentary, or metamorphic origins, but also with respect to their typical texture, or range of textures. This is an important point to note, as both compositional variability as well as origin and geological age control rocktype competence and, hence, all key geo-mechanical parameters.

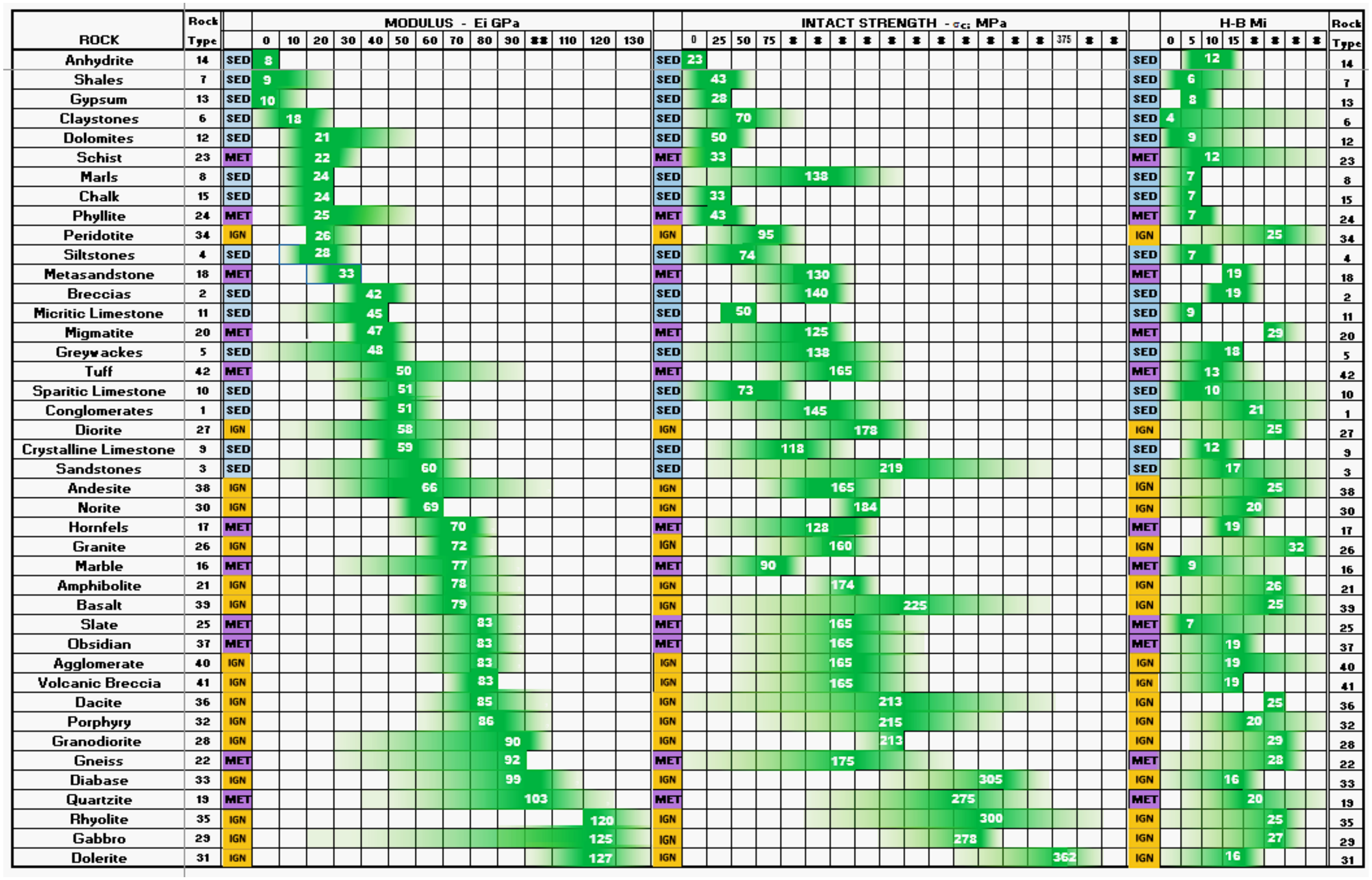

Figure 18: Average values of intact rock modulus Ei, uniaxial compressive strength σci and Hoek-Brown constant mi for various rock types, sorted in terms of increasing rock stiffness. Plot updated from Carter and Marinos, 2020.

Plotting m_i values versus strength σ_{ci} or plotting m_i values versus modulus ratio E_i/σ_{ci} yields plots that show little correlation with rocktype characteristics or mode of origin, as discussed in detail in Carter and Marinos, 2020. The most promising inter-relationships are seen when the 42 rocktypes are sorted by modulus E_i rather than either of the other key parameters, σ_{ci} and m_i, as shown in Figure 16. It is also clear that ranking the rock types by modulus, rather than strength or m_i, sorts the rock types appropriately by origin – the sedimentary rocks almost all showing low stiffness as compared with the igneous rocks at the other end of the stiffness scale, with the metamorphic rocks quite logically distributed right across the spectrum.

Figure 16 is a particularly useful tool during early design stages on a project, when the potential location of a foundation, slope, tunnel, or large underground excavation is being considered, before any detailed core drilling or field mapping has been carried out.

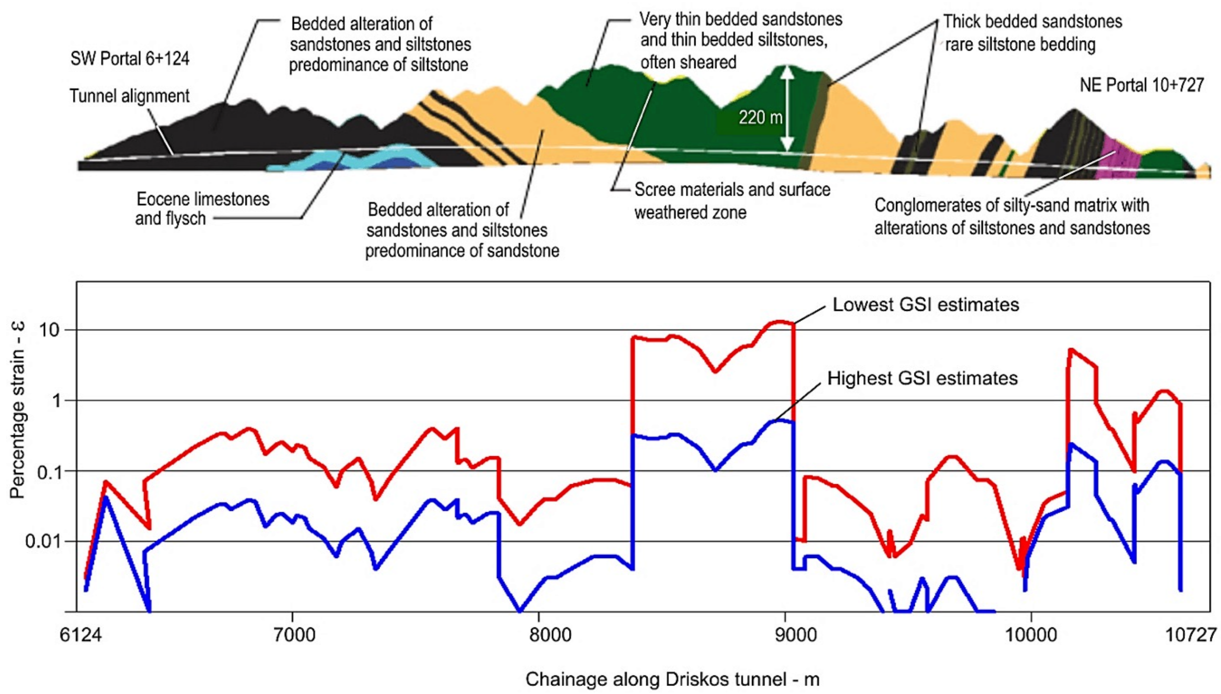

Figure 19: Prediction of potential deformations in the Driskos Tunnel on the Egnatia Highway in Northern Greece. (Percentage strain = (tunnel closure/tunnel diameter) x 100)).

Figure 19 shows the preliminary analysis carried out on the Driskos Tunnel in the Egnatia Highway in Greece. Based on a vey general description of the geology of the potential site, approximate values for the Deformation Modulus, the Uniaxial Compressive Strength, and the Hoek-Brown constant m_i were estimated. Together with the Geological Strength Index (GSI), described in the chapter on rock mass properties, an approximate analysis of the stability and deformation characteristics of the tunnel was carried out. This indicated percentage strains (ratio of tunnel closure to tunnel diameter) of up to 10% in sandstones and siltstones, at a depth of 220 m, in the central portion of the tunnel. Such strains were encountered, during the construction of the tunnel, and these were controlled by the placement of tensioned and grouted multi-strand steel cables before the installation of the final concrete lining.

Acknowledgements

Dr Connor Langford has contributed to the analyses presented in Figures 10 and 12 and Dr Trevor Carter and Dr Vasillis Marinos have contributed to the rock type classifications, plotted in Figures 1 and 18. The assistance of these friends is gratefully acknowledged.

APPENDIX 1: Definition of Sedimentary, Igneous and Metamorphic Rocks

Sedimentary rocks can be considered as being of two types, clastic and non-clastic, as defined in Table 1. The clastic sedimentary rocks typically consist of mineral grains that can vary in size from clays to boulders and at each grain size can also vary significantly in angularity from rounded (sometimes with a high degree of sphericity) to blocky and angular with little rounding, all dependent on degree of comminution involved in their deposition. Like soils, grain size is the predominant divider of rock names within the clastic suite, (ref Table 1, which lists 8 naming divisions, with calcareous mudstone (marl) units included in this suite, although some would argue they should be in the non-clastic grouping). In clastic rocks, individual grains are not always interlocking; rather, mostly they are bonded together by some form of inter-granular matrix cement. Bedding, lamination, and other sedimentation structures in these rocks may create significant anisotropy, with interbedded sequences of alternating argillaceous and arenaceous rocks being the most strongly anisotropic. Some of the more argillaceous rocks, commonly called mudrocks, are susceptible to slaking and in some cases swelling. This group of rocks creates many problems and challenges in rock construction. The non-clastic sedimentary rocks by contrast are formed by various types of chemical precipitation processes that can create rocks that vary in composition from cemented aggregates of bio-organism skeletal fabrics through to almost amorphous crystalline or cryptocrystalline rocks that have interlocked crystal assemblages, similar in many ways to igneous rock crystal geometries. Table 1 gives a guide to further subdivisions of these non-clastic rock types.

Igneous rocks are of two quite different types – *intrusive* – meaning they were injected into the overlying rock units, but formed at depth, only being exposed near surface long after they had solidified; and *extrusive/pyroclastic* – meaning they became exposed on the surface of the earth during their original formation – either as flowing lavas or as ash or other hot ejectamenta derived from a volcanic eruption. Table 1 further divides the intrusive rocks into plutonic and hyperbyssal – reflecting depth of original formation. Both types of rock units tend to be massive and strong with individual crystals essentially welded together as part of their original formation. However, geologists further divide the *intrusive* rocks depending on the mineralogical mix of the original magma, identifying plutonic rocks as either light or dark coloured, but with a typical range of crystal sizes dependent again on the parent mineralogy and the original cooling history. Table 1 outlines the broad subdivisions, with hypabyssal rocks typically always dark.

Mostly, these rocktypes, irrespective of grain size, show complex interlock between crystals, resulting in minor directional differences in mechanical properties. Therefore, good quality aggregates can usually be made from many of these rocktypes and rock engineering construction problems related to *intrusive* rocks in their intact state tend to be minor.

<table>
<tr><th rowspan="2">ROCK TYPE</th><th rowspan="2">CLASS</th><th rowspan="2">GROUP</th><th colspan="4">TEXTURE</th><th rowspan="2">Rock No.</th></tr>
<tr><th>COARSE > 5 mm</th><th>MEDIUM > 0.5 mm</th><th>FINE > 0.05 mm</th><th>VERY FINE</th></tr>
<tr><td rowspan="15">SEDIMENTARY</td><td colspan="2" rowspan="8">CLASTIC</td><td colspan="2">Conglomerates</td><td></td><td></td><td>1</td></tr>
<tr><td colspan="3">Breccias</td><td></td><td>2</td></tr>
<tr><td colspan="3">Sandstones (also Arkoses & Arenites)</td><td></td><td>3</td></tr>
<tr><td></td><td></td><td>Siltstones</td><td></td><td>4</td></tr>
<tr><td></td><td colspan="3">Greywackes</td><td>5</td></tr>
<tr><td></td><td></td><td></td><td>Claystones</td><td>6</td></tr>
<tr><td></td><td></td><td></td><td>Shales</td><td>7</td></tr>
<tr><td></td><td></td><td></td><td>Marls</td><td>8</td></tr>
<tr><td rowspan="7">NON-CLASTIC</td><td rowspan="4">Carbonates</td><td>Crystalline LST</td><td colspan="2">CryptoCrystallIne LST</td><td></td><td>9</td></tr>
<tr><td colspan="2">Sparitic LST</td><td></td><td></td><td>10</td></tr>
<tr><td></td><td></td><td colspan="2">Micritic LST</td><td>11</td></tr>
<tr><td></td><td colspan="3">Dolomites</td><td>12</td></tr>
<tr><td rowspan="2">Evaporites</td><td></td><td colspan="2">Gypsum</td><td></td><td>13</td></tr>
<tr><td></td><td></td><td>Anhydrite</td><td></td><td>14</td></tr>
<tr><td>Organic</td><td></td><td></td><td></td><td>Chalk</td><td>15</td></tr>
<tr><td rowspan="10">METAMORPHIC</td><td colspan="2" rowspan="4">NON-FOLIATED</td><td colspan="2">Marble; (also Skarns)</td><td></td><td></td><td>16</td></tr>
<tr><td></td><td colspan="3">Hornfels</td><td>17</td></tr>
<tr><td>Granulites</td><td colspan="2">Metasandstone</td><td></td><td>18</td></tr>
<tr><td></td><td>Diabase *</td><td colspan="2">Quartzite</td><td>19</td></tr>
<tr><td colspan="2" rowspan="2">SLIGHTLY-FOLIATED (BANDED)</td><td colspan="2">Migmatite</td><td></td><td></td><td>20</td></tr>
<tr><td></td><td colspan="2">Amphibolite</td><td></td><td>21</td></tr>
<tr><td colspan="2" rowspan="4">BANDED/GNEISSOSE FOLIATED SCHISTOSE /CLEAVED</td><td colspan="3">Gneiss</td><td></td><td>22</td></tr>
<tr><td></td><td colspan="2">Schist</td><td></td><td>23</td></tr>
<tr><td></td><td></td><td colspan="2">Phyllite</td><td>24</td></tr>
<tr><td></td><td></td><td></td><td>Slate</td><td>25</td></tr>
<tr><td rowspan="17">IGNEOUS</td><td rowspan="6">PLUTONIC</td><td rowspan="3">FELSIC (Light)</td><td>Granite;</td><td colspan="2">MicroGranite</td><td>Aplite</td><td>26</td></tr>
<tr><td></td><td>Diorite</td><td colspan="2">MicroDiorite</td><td>27</td></tr>
<tr><td colspan="2">Granodiorite</td><td></td><td></td><td>28</td></tr>
<tr><td rowspan="3">MAFIC (Dark)</td><td colspan="2">Gabbro</td><td></td><td></td><td>29</td></tr>
<tr><td>Norite</td><td></td><td></td><td></td><td>30</td></tr>
<tr><td>Syenite</td><td colspan="2">Dolerite</td><td></td><td>31</td></tr>
<tr><td rowspan="3">HYPABYSSAL</td><td rowspan="3">ULTRABASIC</td><td colspan="2">Porphyry and Dunite</td><td></td><td></td><td>32</td></tr>
<tr><td></td><td colspan="2">Diabase* and Eclogite</td><td></td><td>33</td></tr>
<tr><td></td><td colspan="3">Pyroxenite and Peridotite</td><td>34</td></tr>
<tr><td rowspan="8">VOLCANIC</td><td rowspan="5">EXTRUSIVE (Lava)</td><td></td><td></td><td colspan="2">Rhyolite</td><td>35</td></tr>
<tr><td></td><td>Trachyte</td><td>Dacite</td><td></td><td>36</td></tr>
<tr><td></td><td></td><td></td><td>Obsidian >></td><td>37</td></tr>
<tr><td></td><td colspan="2">Andesite</td><td></td><td>38</td></tr>
<tr><td colspan="3">Basalt</td><td></td><td>39</td></tr>
<tr><td rowspan="3">PYROCLASTIC</td><td colspan="2">Agglomerate</td><td>Ignimbrite</td><td></td><td>40</td></tr>
<tr><td colspan="3">Volcanic Breccia</td><td></td><td>41</td></tr>
<tr><td></td><td></td><td colspan="2">Tuff</td><td>42</td></tr>
</table>

*Diabase = Dolerite per N.American nomenclature; = Metamorphosed Dolerite (European nomenclature)

Table 1: Textural and origin-based classification of common rock types (Plot courtesy of Dr. Trevor Carter, 2021).

Geologically young (eg. Tertiary to Cretaceous < 100my) *extrusive* igneous rocks, by contrast, can be extremely problematic, as almost all, including even the most competent units may contain deleterious mineralogy, which, with weathering, can break down sometimes to swelling clays. The most problematic young extrusive rocks are the gassy lavas – mainly these occur just amongst the andesites, while almost all the pyroclastics can be troublesome, especially the tuffaceous (ash, scoria, etc.) rock units, except sometimes when welded. The volcaniclastic group of rocks are amongst the most problematic of all. These rock types, which originated as pyroclastic origin deposits that ended up falling into water and then being deposited as sediments, under the same processes as the sedimentary rocks, can look like sedimentary rock and exhibit all the same characteristics, but contain deleterious mineralogy and, hence, exhibit inferior engineering properties compared with their normal pure sedimentary counterparts. Great care must therefore be taken when constructing in, or on, any of these types of volcanic rock units. Such construction difficulties may not be such a problem in geologically much older rocks of the same names – such as might occur in the Cambrian or Archean, 600-6000 million years as with induration and even light metamorphism many of these problematic characters become much less prevalent or may even be completely absent.

Metamorphic rocks are so named because they have been changed from their original character by pressure or temperature, or both. This results in many different fabrics, which is what geologists typically use as the primary descriptor when naming a metamorphic rock. The second descriptor is mineralogy, as certain suites of minerals are only found in certain specific pressure and temperature ranges. The full suite of metamorphic rock types listed in Table 1 can be found in areas of *Regional Metamorphism* but may not always be present when dealing with areas of *Contact Metamorphism* (such as may occur around an igneous intrusion, or an ore emplacement zone, due to baking of the country rock), as quite commonly seen around many deposits being exploited by both surface and underground mining. Both processes can create a wide range of different metamorphic rock fabrics depending on the original starting rocktype. It is surprising how many of the world's rocks are metamorphosed to some degree. Layered gneisses and schists of various geological ages, right back to the Archean are extremely common worldwide, as they generally represent the metamorphosed equivalents of original arenaceous and argillaceous clastic sedimentary rock units. Shales, (ie., fissile mudstones), which are also common worldwide, are typically grouped in with the sedimentary rock units (ref. Table 1), but really should be included as metamorphic rocks as they are essentially the product of very low-grade pressure (consolidation) metamorphism. By contrast hornfels and granulite metamorphic rocks, which are less widespread can be quite amorphous and exhibit quite good engineering properties compared with the more foliated metamorphic rock types, notably the schists. Taken overall, metamorphic rocks can show as wide as, or wider, range in structure and composition and properties as the sedimentary rocks. Some of the highest-grade metamorphic processes result in near melting and annealing occurring, thus generating rocks of high competence and high intact rock strength, devoid of any of anisotropy common amongst all the other metamorphic rocks of lower grade. At lower grades preferred orientation of platy (sheet) minerals results in considerable directional differences in mechanical properties. Micaceous and chloritic schists are amongst the most anisotropic from the viewpoint of strength and stiffness contrasts, while slates are not mineralogically as variable as schists, yet exhibit an extreme fabric anisotropy created by pressure induced cleavage throughout the rock.

APPENDIX 2: Diamond core sampling, storage, and preparation

Figure A1 illustrates a compact drill rig, suitable for use on surface and in relatively small sized tunnels. There are many variations of this type of drill and, with correct set up and operating procedures, they produce high quality core which is suitable for testing to determine the strength and deformation properties of the intact rock.

Typically, the core size chosen for geotechnical testing is 47.6 mm in diameter and is designated as NQ core. However, a wide range of core sizes is available to researchers with other requirements. In general, it is advisable to consult a geotechnical engineer or specialist contractor on setting up a site investigation program since costly mistakes can occur if such a program is not well planned and executed.

Once the core has been recovered, geotechnical logging and storage of the core are critical requirements. Figure A2 shows a series of cores recovered from an exploration site for a large open pit copper mine on a site with no surface exposure of the potential orebody. Hence, all information on both the mineral content and the geotechnical properties of the orebody, and the surrounding rock, had to be determined from the core.

Figure A1: A compact diamond drill rig that can be used for drilling from surface or in a tunnel.

Figure A2: Diamond drilled core, for both mineral exploration and geotechnical properties, laid out for logging.

Figure A3: A storage facility for diamond drilled core for geotechnical investigations.

A very well-designed storage facility for diamond drilled core is illustrated in Figure A3. The core is stored in closed core boxes which, in turn, are stored on numbered shelves in the storage sheds. Hence, the core is protected from exposure and yet, is easy to access when required for inspection.

In contrast, inappropriate core storage is illustrated in Figures A4 and A5. Given the high cost of the diamond drilling process and the potential loss of valuable information, treatment of core in this manner is unacceptable.

Figure A4: Inappropriate core storage in a tropical environment.

Figure A5: Security is essential to prevent tampering and vandalism of core storage facilities.

In some situations, such as that illustrated in Figure A6, unusual steps may have to be taken to recover reliable geotechnical information. In this case, the site investigations were being carried out for the design of a large underground cavern in a hydro-electric project. The rock mass in which the cavern was excavated consisted of a sedimentary series of inter-bedded sandstone, siltstone, and shale. As shown on the right of the photograph, the siltstone and shale deteriorated quickly due to changes in moisture content when it was removed from its in-situ environment. This required that geotechnical testing of the core had to be carried out as soon as possible after drilling, preferably on site. It also necessitated a change in the basic design of the cavern support system in that shotcrete had to be applied to exposed rock surfaces, as soon as possible after excavation, to prevent deterioration and loss of strength of the rock in the cavern walls.

Figure A6: Diamond drilled core samples through a sedimentary sequence consisting of inter-bedded sandstone, siltstone and shale. Freshly drilled core is shown on the left while, on the right, is core that has been stored in a core shed for six months. Deterioration of the mudstone and shale in the centre of the core box is due to changes in moisture content.

The next stage in the geotechnical investigation process is to prepare the core specimens for testing to determine the strength and deformation characteristics of the intact rock. This involves cutting specimens from the core and preparing these specimens for loading in the equipment to be described in the following pages. Typically, the length of each specimen should be a minimum of twice its diameter. The American Institute of Mining, Metallurgical, and Petroleum Engineers and the International Society for Rock Mechanics and Rock Engineering recommend a length to diameter ratio of 2.5 to 3 for the testing of core samples. Both ends of the specimen should be perpendicular to the core axis and perfectly flat.

All the steps required for the preparation of the specimens to meet these requirements can be performed using a conventional metal cutting and turning lathe, as illustrated in Figures A7 to A12. The most important addition to the lathe is a toolpost grinder on which a range of diamond-impregnated steel cutting tools can be attached.

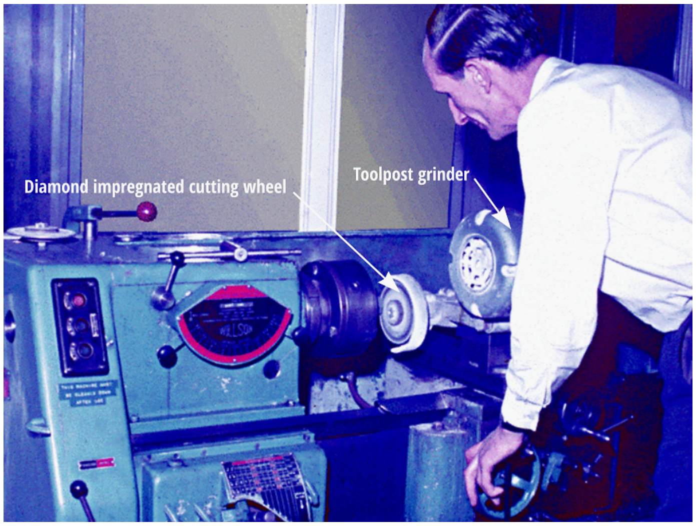

Figure A7: A lathe, equipped with a toolpost grinder mounted on the cross slide, can be used to perform all the preparations required for testing diamond drilled core samples of intact rock.

Figure A8: Cutting through a core specimen using a diamond impregnated steel cutting disc, mounted on a toolpost grinder as shown in Figure 7. Water can generally be used for cooling but, for sensitive soft rock, air should be used.

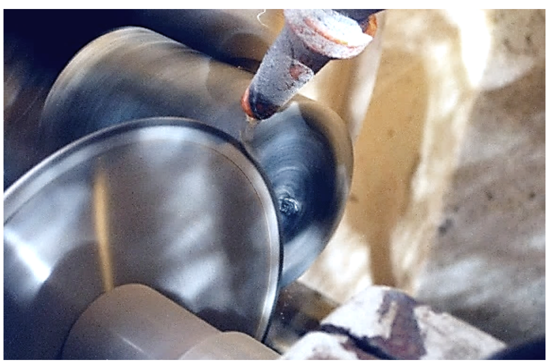

Figure A9: Cutting the dimple off the end of a core specimen by running the diamond impregnated cutting blade across the centre of the core.

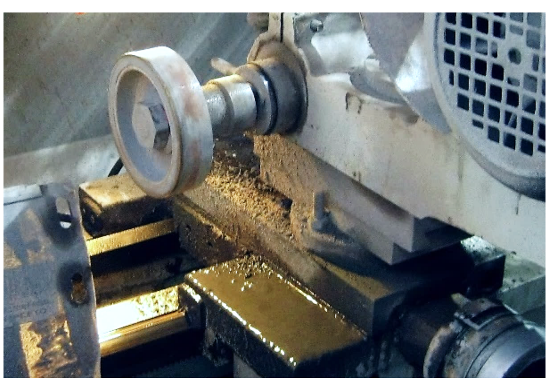

Figure A10: Where necessary, the final trimming of the ends of the core specimen can be done by running the diamond impregnated surface of a cup-shaped grinding wheel across the centre of the specimen.

Figure A11: Rock core end flatness tester.

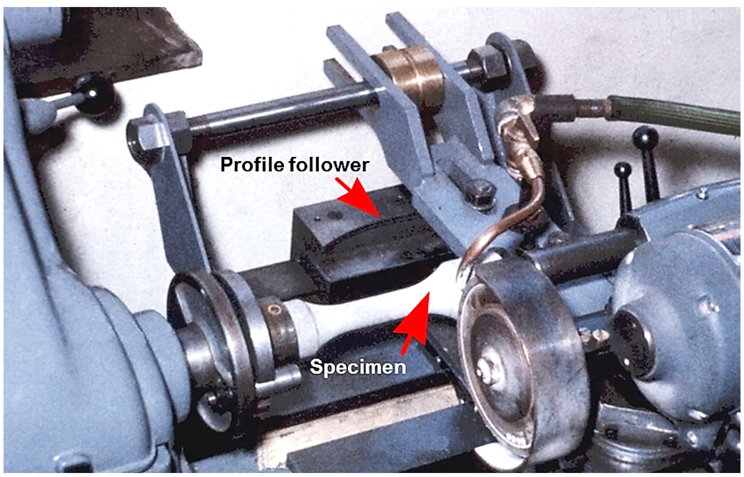

Figure A12: Preparation of a dog-bone shaped specimen for confined tensile testing can be done by using a profile follower which guides the diamond blade mounted on a toolpost grinder to form the required shape.

In addition to the preparation of cylindrical core specimens with flat ends, as described above, the lathe can also be used to machine dog-bone or dumb-bell shaped specimens such as that illustrated in Figure A12. In this case, one end of the diamond drilled core is mounted in the lathe chuck while the other end is held in a cup which rotates in a roller bearing attached to the tailstock of the lathe. The toolpost grinder is guided to cut the recessed shape in the core by a profile follower such as that illustrated in Figure A12. Specimens of this shape are used for confined tensile testing, as described in a section of this chapter.

Triaxial testing of intact rock specimens

Triaxial compression testing of the flat ended core specimens, prepared as described above, can be carried out in a triaxial cell such as that illustrated in Figure A13. Details of the design and construction for this cell can be found in papers by Hoek and Franklin (1968) and Franklin and Hoek (1970). Testing machines used to apply the axial loads to the specimens range from relatively simple equipment, such as that illustrated in Figure A14, to more sophisticated equipment such as that shown in Figures A15 and A16. Careful preparation of the specimens and the testing procedures can ensure that the results obtained using any of the equipment illustrated will meet the highest standards required for practical applications in rock engineering.

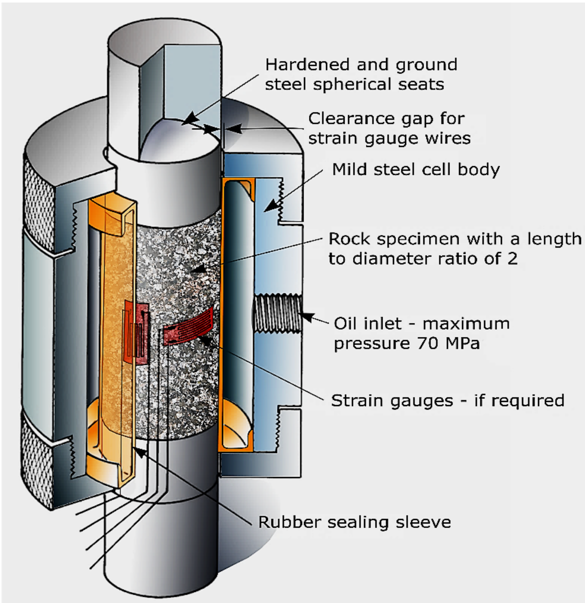

Figure A13: Cut-away view of a triaxial cell for subjecting laterally confined specimens to axial loading.

Figure A14: A small field laboratory on a large open pit mine project. High quality uniaxial and triaxial testing can be carried out in such a laboratory.

Figure A15: Controls Group semi-automatic equipment for uniaxial and triaxial testing of rock specimens with limited data acquisition capability.

Figure A16: Controls Group equipment for triaxial testing of rock specimens with full data acquisition capability.

References

Arshadnejad, S. 2018. Determination of "*mi*" in the Hoek-Brown failure criterion of rock. *Mining Science*. 25, 111-117.

Balmer, G. 1952. A general analytic solution for Mohr's envelope. Paper POR1952-5. *ASTM Proceedings* 1952, 52. 1260-1271.

Bewick, R. P., Amann, F., Kaiser, P. K., & Martin, C. D. (2015). Interpretation of UCS Test Results for Engineering Design. Proceedings 13th International Congress of Rock Mechanics - ISRM Congress 2015, Montreal, 1-14.

Bewick, R. P., Kaiser, P. K., & Amann, F. (2019). Strength of massive to moderately jointed hard rock masses. Journal of Rock Mechanics and Geotechnical Engineering, 11, 562-575.

Bobich, J.K. 2005. Experimental analysis of the extension to shear fracture transition in Berea sandstone. *MS thesis*. Texas A & M University.

Brace, W.F., 1964. Brittle fracture of rocks. *In State of Stress in the Earth's Crust*. W.R. Judd (ed.), New York: Elsevier, 111-174.

Byerlee, J.D., 1968. Brittle-Ductile transition in rocks. *Journal of Geophysical Research*. 73, 14.

Carter, T.G., and Marinos, V. 2020. Putting geological focus back into rock engineering design. *Rock Mech Rock Eng* Vol. 53(10):4487–4508.

Carter, T.G., 2021. Towards Improved Definition of the Hoek-Brown Constant mi for Numerical Modelling, *Paper RICAB84, Rocscience International Conference 2021*, 20-21.

Carranza-Torres, C.T. and Corkum, B. 2002. Hoek-Brown Failure Criterion— 2002 Edition. *Proceedings of the 5th North American Rock Mechanics Symposium*, Toronto, July 2002, 267-273.

Chakraborty, S., Bisal, R., Palaniappon, S.K. and Pal, S.K. 2019. Failure modes in rock under uniaxial compression tests: an experimental approach. *Journal of Advances in Geotechnical Engineering*, Vol. 2, No. 3.

Evans, B., Fredrich, J.T. and Wong, T-F. 2013. The Brittle-Ductile Transition in Rocks: Recent Experimental and Theoretical Progress, in *The Brittle-Ductile Transition in Rocks: The Heard Volume*, Editors: A. G. Duba, W. B. Durham , J. W. Handin , H. F. Wang, American Geophysical Union. 1-20.

Fairhurst C. 1964. On the validity of the "Brazilian" test for brittle materials. *International Journal of Rock Mechanics and Mining Sciences.* 4, 535-46.

Franklin, J.A. and Hoek, E. 1970. Developments in triaxial testing equipment. *Rock Mech*. **2**, 223-228.

Griffith, A.A. 1924. The theory of rupture, *Proc. Int. Congr. Appl. Mech*. 56-63.

Hoek, E. 1964. Fracture of anisotropic rock. *Journal of the South African Institute of Mining and Metallurgy* 10, 501-518.

Hoek, E. 1965. Rock fracture under static stress conditions. *CSIR Report MEG. 1965*. p. 383.

Hoek E. & Franklin J.A, 1968. Simple Triaxial Cell for Field or Laboratory Testing of Rock. *Trans. Inst. Min. Metall*. A22-26.

Hoek, E., and Brown, E.T. 1980. *Underground excavations in rock*. London: Instn Min. Metall.

Hoek, E., and Brown, E.T. 1980. Empirical strength criterion for rock masses. *J. Geotech. Engng Div*., ASCE,106 (GT9),1013-1035.

Hoek, E., and Brown, E.T. 2019. The Hoek-Brown failure criterion and GSI – 2018 edition. *Journal of Rock Mechanics and Geotechnical Engineering.* 11, 3, 445-463.

Hoek, E. 1999. Putting numbers to geology – an engineer's point of view. *Quarterly Journal of Engineering Geolog*y, 32, 1, 1-19.

Hoek, E., Carranza-Torres, C. and Corkum, B. 2002. Hoek-Brown criterion – 2002 edition. In *5th North American Rock Mechanics Symposium.* Toronto, 7-10 July 2002. Eds. R. Hammah et al. 267-73. Toronto, University of Toronto Press.

Hoek, E. and Diederichs, M.S. 2006. Empirical Estimation of Rock Mass Modulus. I*nternational Journal of Rock Mechanics and Mining Sciences*, 43, 203-215.

Hu, K., Zhu, Q.Z, Chen, L, Shao, J.F. and Liu, J. 2018. A micromechanics-based elastoplastic damage model for rocks with a brittle–ductile transition in mechanical response, *Rock Mechanics and Rock Engineering*, 51, 6, 1729–1737.

Keyter, G.J., Ridgeway, M. and Varley, P.M. 2008. Rock Engineering aspects of the Ingula Powerhouse caverns. *Proc. 6th International Symposium on Ground Support in Mining and Civil Engineering Construction.* SAIMM, 309-445.

Judd, W. R. 1964. Proc. Intnl. Conf. on the State of Stress in the Earth's Crust. Santa Monica, ed. W. R. Judd. Elsevier Publishing Co., New York, 1964.

Mogi, K., 1966. Pressure dependence of rock strength and transition from brittle ductile flow, *Bull. Earthquake Res. Inst.* Tokyo Univ. 215-232.

Murrell, SAF, 1965. The effect of triaxial stress systems on the strength of rocks at atmospheric temperatures, *Geophysical Journal International*, 3, 231-281.

Palmström, A., 1995. RMi – a rock mass characterization system for rock engineering purposes. *PhD* thesis, Oslo University, Norway, 400 pages.

Perras, M.A. and Diederichs, M.S. 2014. A Review of the Tensile Strength of Rock. Concepts and Testing, Geotechnical and Geological Engineering. 32(2), 525-546.

Ramsey, J. and Chester, F. 2004. Hybrid fracture and the transition from extension fracture to shear fracture, *Nature, 428,* 63-66.

Scholz, C.H., 1968. Microfracturing and the inelastic deformation of rock in compression, *Journal of Geophysical Research*, 73, 4, 1417–1432.

Schwartz, A. E., 1964. Failure of rock in triaxial shear. *Proc. 6th Rock Mechanics Symposium.* Rolla, Missouri. 109-135.